Water hammer protective performance of a spherical air vessel caused by a pump trip

Lin Shi, Jian Zhang, Xiaodong Yu and Sheng Chen

ABSTRACT

The use of air vessels is an effective measure to control water hammer in a long-distance water supply system. The traditional shape of such vessels is cylindrical. In this paper, an innovative spherical air vessel is proposed to improve the force characteristics of the tank. A mathematical model of the spherical air vessel was established using the method of characteristics. A comparison was performed of water-hammer protection performance between the spherical air vessel and the cylindrical air vessel based on a practical water supply project. Furthermore, a sensitivity analysis on the parameters of the spherical air vessel was performed. The results showed that the spherical air vessels had better protective performance compared with the cylindrical air vessels. Under the same protection requirements, the spherical air vessel can reduce the total volume and surface area by more than 10%. In addition, for a fixed volume of the spherical air vessel, the protective effect improves with the increase of the initial gas volume. Increasing the connecting pipe diameter of the air vessel is beneficial for low-pressure protection, whereas it is adverse to high-pressure protection; in contrast, altering the installation elevation has little effect on water-hammer protection.

Key words | long-distance water supply, pump trip, sensitivity analysis, spherical air vessel, water hammer

Lin Shi
Jian Zhang
Xiaodong Yu (corresponding author)
Sheng Chen
College of Water Conservancy and Hydropower Engineering,
Hohai University,
Nanjing 210098,
China
E-mail: *yuxiaodong_851@hhu.edu.cn*

INTRODUCTION

A long-distance water supply project is an effective method to reallocate and improve the utilization of water resources. Pipeline safety issues are major challenges in a long-distance water supply system with pump stations. A pump-stopping water hammer is generated when the pump suddenly stops. The points where the initial pressures are relatively low along the pipeline may be reduced to the vaporization pressure, thereby causing the column separation phenomenon to occur. The enormous pressure generated by the column separation water hammer may cause huge damage to the pipeline system and result in interruption of the water supply (Bergant *et al.* 2006).

Air vessels have been developed and successfully used to overcome these problems because they can be conveniently installed and managed. Generally, the performance of an air vessel mainly depends on its total volume, initial gas volume, connecting pipe diameter etc. (Miao *et al.* 2017), and an air vessel with large volume can often achieve better water-hammer protection. However, an overlarge volume may lead to more engineering investment. Many previous studies have focused on the influence of the ratio of gas volume on the volume of air vessels (Kim *et al.* 2014; Besharat *et al.* 2017). In addition, several researchers have worked on the effect of the connection configuration on water-hammer protection performance, and different types of connection configurations have been proposed (Stephenson 2002; Sun *et al.* 2016). Taking a different perspective on those previously mentioned, He *et al.* (2017) proposed a horizontal air vessel and found that the horizontal air vessel had a relatively better protective performance than the vertical one. Wang *et al.* (2013) investigated the protection effect of installation position on

doi: 10.2166/ws.2019.063

water hammer and concluded that the air vessel should be close to the outlet of the pump to obtain better protection effects.

However, the studies described above for air vessels, regardless of connection configuration, ratio of air volume, mounting style, or installation position, are for cylindrical structures. Few studies have focused on the effect of parameters related to the geometry of the structures of the air vessels. A vessel is generally made into a spherical structure in industrial fields because of its good force characteristics and bearing capacity (Perl & Perry 2010). In light of this background, the purpose of this paper is to evaluate the influence of the spherical air vessel on water-hammer protection according to the good mechanical properties of the spherical structure. A mathematical model of a spherical air vessel is established based on the method of characteristics (MOC) (Wylie *et al.* 1993). Cylindrical and spherical air vessels are used to protect from pump-stopping water hammer in a practical project, and the protective effects of these two air vessels are compared using numerical simulation methods. A sensitivity analysis regarding the initial gas volume, the connecting pipe diameter, and the installation elevation of the spherical air vessel is presented as well.

MATHEMATICAL MODEL

Schematics of the conventional cylindrical air vessel and the spherical air vessel structures are shown in Figure 1. The upper parts of the vessels are filled with highly pressurized gas, whereas the lower parts are full of water. The bottoms of the vessels are connected to the main conduits via short pipes.

The mathematical model of the spherical air vessel is shown in Figure 1(b). It is assumed that the gas in the vessel is ideal and water elasticity is neglected. In Figure 1(b), Q_{P1} is the discharge in front of the node of the air vessel (m^3/s); Q_{P2} is the discharge behind the node of the air vessel (m^3/s); Q_{st} is the discharge flowing into or flowing out of the air vessel, and Q_{st} is positive when water flows into the vessel and is otherwise negative (m^3/s); Z_{st} is the water level in the air vessel (m); H_C is the height of the center of the sphere of the spherical vessel (m); L_s is the diameter of the water cross-section in the vessel (m); and R is the radius of the spherical vessel (m). The compatibility equations are given by Equation (1):

$$\begin{cases} H_P = C_{P1} - B_{P1}Q_{P1} \\ H_P = C_{M2} + B_{M2}Q_{P2} \end{cases} \tag{1}$$

where C_{P1}, B_{P1}, C_{M2}, and B_{M2} are all known at time t–Δt, and Δt is the time step; H_P is the pressure at the connection point between the air vessel and the pipeline (m). The energy equation and the continuity equation can be written as Equations (2) and (3), respectively. The relationship between water level and flow rate in the air vessel is shown in Equation (4). Moreover, the enclosed air at the upper portion of the tank follows the polytropic relationship given by Equation (5).

$$H_P = Z_{st} + \frac{p - p_0}{\gamma} + kQ_{st}|Q_{st}| \tag{2}$$

$$Q_{P1} = Q_{st} + Q_{P2} \tag{3}$$

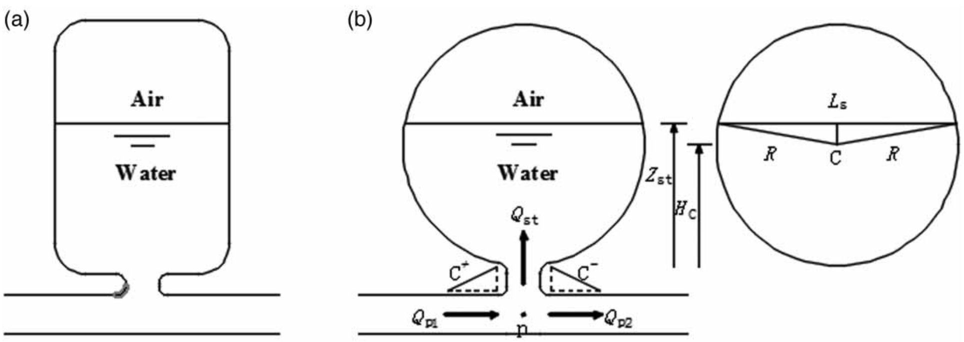

Figure 1 | Schematics of the air vessel: (a) cylindrical air vessel; (b) spherical air vessel.

$$A_{st}\frac{dZ_{st}}{dt} = Q_{st} \tag{4}$$

$$pV_{air}^{n} = C \tag{5}$$

where p is the absolute pressure of gas in the air vessel (Pa); p_0 is the local atmospheric pressure (Pa); k is the hydraulic loss coefficient at the connection point between the air vessel and the pipeline; A_{st} is the cross-sectional area of the water surface in the air vessel (m^2); V_{air} is the gas volume in the air vessel (m^3); n is the exponent in the polytropic gas equation and C is a constant. The value of n is 1.0 and 1.4 for an isothermal and adiabatic expansion or contraction of the air, respectively. In this calculation $n = 1.2$ was taken because the transients are usually rapid at the beginning but slow near the end (Chaudhry 2014).

Considering the time step Δt is small, Equations (2) and (4) are integrated and the second-order approximation is taken; thus, Equations (6) and (7) are obtained as below:

$$H_P = Z_{st} + \frac{p - p_0}{\gamma} + kQ_{st}|Q_{st0}| \tag{6}$$

$$\Delta Z = Z_{st} - Z_{st0} = \frac{(Q_{st} + Q_{st0})\Delta t}{2A_{st0}} \tag{7}$$

where Z_{st0} , Q_{st0}, A_{st0}, and V_{air0} are all known quantities at time t–Δt.

From the geometric relationship in Figure 1(b), the water cross-section diameter can be written as Equation (8). Thus, the sectional area of the water surface and the gas volume of the air vessel can be expressed as Equations (9) and (10).

$$L_s = 2\sqrt{R^2 - (Z_{st} - H_C)^2} \tag{8}$$

$$A_{st} = \pi(R^2 - (Z_{st} - H_C)^2) \tag{9}$$

$$V_{air} = \frac{\pi}{3}(R + H_C - Z_{st})^2(2R - H_C + Z_{st}) \tag{10}$$

Using Taylor series expansion, Equation (5) can be written as Equation (11). Considering that the size of the time step Δt is small, Equation (5) can be simplified as Equation (12). Thus, taking Equations (1), (3), (7) and (12) into Equation (6), the bottom pressure of the air vessel can eventually be described as Equation (13).

$$pV_{air0}^{n}\left[1 - \frac{nA_{st0}}{V_{air0}}(Z_{st} - Z_{st0})\right] = C \tag{11}$$

$$p = C_1 + C_2\Delta Z \tag{12}$$

$$H_P = \frac{C_3 + C_4\left(\frac{C_{P1}}{B_{P1}} + \frac{C_{M2}}{B_{M2}}\right)}{1 + C_4\left(\frac{1}{B_{P1}} + \frac{1}{B_{M2}}\right)} \tag{13}$$

where $C_1 = \frac{C}{V_{air0}^{n}}$, $C_2 = \frac{nC_1A_{st0}}{V_{air0}}$, $C_3 = Z_{st0} + \frac{C_1 - P_0}{\gamma} + \left(1 + \frac{C_2}{\gamma}\right)\frac{Q_{st0}}{2A_{st0}}\Delta t$, $C_4 = \left(1 + \frac{C_2}{\gamma}\right)\frac{\Delta t}{2A_{st0}} + k|Q_{st0}|$

CASE STUDY

The case study considered was a pumping water supply system, conveying water to a downstream tank, with the length of the pipeline 10 km, and the total design water discharge 0.2 m^3/s. The design water level of the suction sump was 1,198.5 m, and that of the outlet sump was 1,294 m. The material of the pipeline was nodular cast iron, and the pipe diameter was 500 mm. Two horizontal centrifugal pumps were installed, of which one pump was the backup unit. The water-hammer wave velocity in the pipeline was 1,000 m/s. The other parameters in the system are listed in Table 1.

Figure 2 shows a schematic of the water supply system with the spherical air vessel. The spherical air vessel was located adjacent to the pump. To avoid water backflow to the pump, a check valve was provided between the air vessel and the pump. Moreover, negative pressure along the pipeline was not allowed when the power failure occurred in this project, and the maximum internal water pressure was not to exceed 160 m.

To compare the protective effects of the cylindrical and spherical air vessels, the following three cases were adopted for this paper. Case 1 is the use of a cylindrical air vessel as the protective measure. Here, the cylindrical air vessel is denoted as C1. Case 2 involves the use of a spherical air

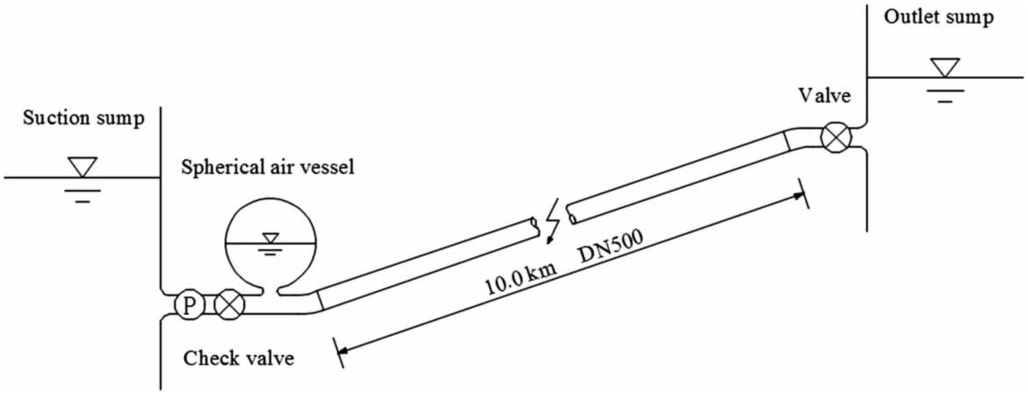

Figure 2 | Schematic of the water supply system with the spherical air vessel.

Table 1 | Parameters of the pipeline system

Pump head (m)	Flow discharge (m^3/s)	Rated speed (r/min)	Motor inertia (kg·m^2)	Pump inertia (kg·m^2)	Motor power (kW)	Roughness coefficient
120	0.2	1,450	44.3	5.7	350	0.012

vessel with the same total volume as in Case 1. Here, the spherical air vessel is denoted as S1. Case 3 involves the use of a cylindrical air vessel with the same protection effect as Case 2. Here, the cylindrical air vessel is denoted as C2. The check valve would be completely closed in 2 s when a pump trip occurred, and a safe water depth in the air vessel was observed under any conditions to avoid gas leakage. With these conditions, the optimized air vessel parameters are shown in Table 2. The MOC was also used to simulate the pump trip water hammer based on these data.

RESULTS AND DISCUSSION

Assuming no water-hammer protective measures were taken in the water supply system, the maximum and minimum pressure curves along the pipeline are shown in Figure 3(a). Figure 3(a) shows that most of the minimum pressures along the pipeline were below the vaporization pressure (−10 m) if no protective measures were placed in the system. Moreover, approximately half of the maximum pressures along the pipeline were above 160 m. In contrast, all the minimum pressures along the pipeline were above 0 m and the maximum pressures were below 160 m with the protection of C1, C2 and S1, as shown in Figure 3(a). This behavior occurred because the pressure and discharge behind the pump began to decrease when the pump stopped suddenly. Subsequently, the high-pressure gas in the vessel expanded quickly to keep the pressure balanced between the vessel and the pipeline. The expanding gas forced the water to flow from the vessel into the pipeline; thus, the water-hammer propagation between the pump and the pipeline was cut off, consequently contributing to the effective protection of the pump as well as the water supply pipeline.

Table 2 | Parameters of the air vessels

Case	Water depth (m)	Air height (m)	Cross-sectional diameter (m^2)	Initial absolute pressure (m)	Connecting pipe diameter (m)	Surface area (m^2)	Total volume (m^3)
Case 1	1.30	1.00	3.14	133.10	0.40	20.73	7.22
Case 2	1.20	1.20	4.52	133.10	0.40	18.10	7.23
Case 3	1.30	1.00	3.60	133.10	0.40	21.75	8.28

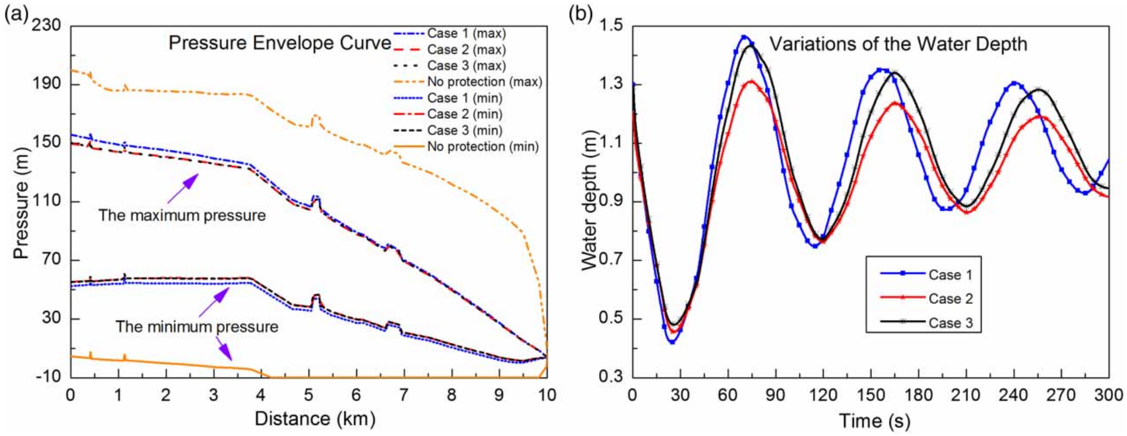

Figure 3 | The calculations for different cases.

Therefore, both the cylindrical and spherical air vessels can effectively prevent pipeline damage caused by water hammer, which verified the previous studies that the air vessel can effectively reduce water hammer in the water supply system (Lee 1998; Liang *et al.* 2005).

Figure 3(b) shows plots of the variations of water depth for Case 1, Case 2 and Case 3. The water depths in the vessels for the three cases were reduced to the minimum at approximately 28 s, and the minimum safe water depths were similar, indicating that the safety margins of these air vessels were the same. The water level in the vessels rose to the maximum at approximately 76 s. The maximum water depths of Case 1 and Case 3 were similar, whereas that of Case 2 was significantly smaller than those of Case 1 and Case 3. Thus the amplitude of the water level fluctuation in the spherical air vessel was smaller than that in the cylindrical air vessel. The reason that could explain the difference is that the water cross-sectional area of the spherical air vessel near the sphere center is larger than that of the cylindrical air vessel.

The volumes of C1 in Case 1 and S1 in Case 2 were the same, but the minimum pressure along the pipeline of S1 was higher than that of C1, and the maximum pressure along the pipeline was lower than that of C1, as shown in Figure 3(a). The water level fluctuation in the spherical air vessel is significantly less than that in the cylindrical air vessel because of its larger water cross-sectional area. According to the energy equation, the bottom pressure variation caused by the change of water level in the spherical air vessel is smaller than that in the cylindrical air vessel. Previous work showed that reducing the bottom pressure variation in the air vessel is beneficial for water-hammer protection (Deng *et al.* 2015). The same conclusion exists in this paper. In contrast, the water cross-sectional area of the spherical air vessel is relatively small as it approaches the bottom. Therefore, with the same volume and the same safe water depth, the spherical air vessel provides more water supply to the pipeline; as a result, the ability to prevent pipeline pressure drop is improved. Moreover, the surface area of S1 was reduced by 12.7% compared with C1, as shown in Table 2.

As for S1 in Case 2 and C2 in Case 3, the maximum and minimum pressure envelope curves along the pipeline were found to be almost coincident with the protection of S1 and C2 (i.e., the protection effect of S1 and C2 on water hammer were the same). However, the total volume of S1 was reduced by 12.7% and the surface area was reduced by 16.78% compared with C2 under these conditions, as shown in Table 2. Accordingly, it can be finally concluded that the spherical air vessel has both good bearing capacity and great effectiveness in reducing the total volume and the surface area of the vessel under the premise of meeting the protection requirements in the water supply system.

SENSITIVITY ANALYSIS

In general cases, the air vessel with large initial volume can often achieve better water-hammer protection. However, the size of the air vessel is affected by economic factors for actual engineering programs. If the total volume is fixed, then the design parameters, such as initial gas volume,

Table 3 | Parameters of different spherical air vessels

Air vessel	D (m)	h (m)	d (m)	El (m)	V (m³)
S2	2.40	$h_2 = 1.10$	0.40	1,193.60	7.23
S3	2.40	$h_3 = 1.20$	0.40	1,193.60	7.23
S4	2.40	$h_4 = 1.30$	0.40	1,193.60	7.23
S5	2.40	1.20	$d_5 = 0.24$	1,193.60	7.23
S6	2.40	1.20	$d_6 = 0.32$	1,193.60	7.23
S7	2.40	1.20	$d_7 = 0.40$	1,193.60	7.23
S8	2.40	1.20	0.40	$El_8 = 1{,}190.60$	7.23
S9	2.40	1.20	0.40	$El_9 = 1{,}193.60$	7.23
S10	2.40	1.20	0.40	$El_{10} = 1{,}196.60$	7.23

connecting pipe diameter and installation elevation of the air vessel, have an important influence on the protection performance from water hammer. The following section takes the long-distance water supply engineering mentioned above as an example to investigate the influences of the behaviors of different parameters on the water-hammer protection effect. The specific parameter values of the spherical air vessel are shown in Table 3, where D = diameter of spherical air vessel; h = air height; d = connecting pipe diameter; El = installation elevation; V = volume of air vessel.

Figure 4(a) presents the maximum and the minimum pressure along the pipeline as a function of both h and *distance*. In Figure 4(a), the maximum pressures along the pipeline decreased with the increase of the air height, whereas the minimum pressures were just the opposite. The calculations indicated that increasing the initial gas volume in the vessel is beneficial for water-hammer protection. Based on Equation (5), the influence of the gas volume variation on the absolute gas pressure decreased with the rise of the initial gas volume in the vessel; thus, the pressure amplitude at the bottom of the vessel decreased, i.e., the air vessel provided an improved water-hammer protection effect. However, increasing the initial gas volume is bound to reduce the water volume in the vessel. Therefore, increasing the initial gas volume can achieve an improved water-hammer protection

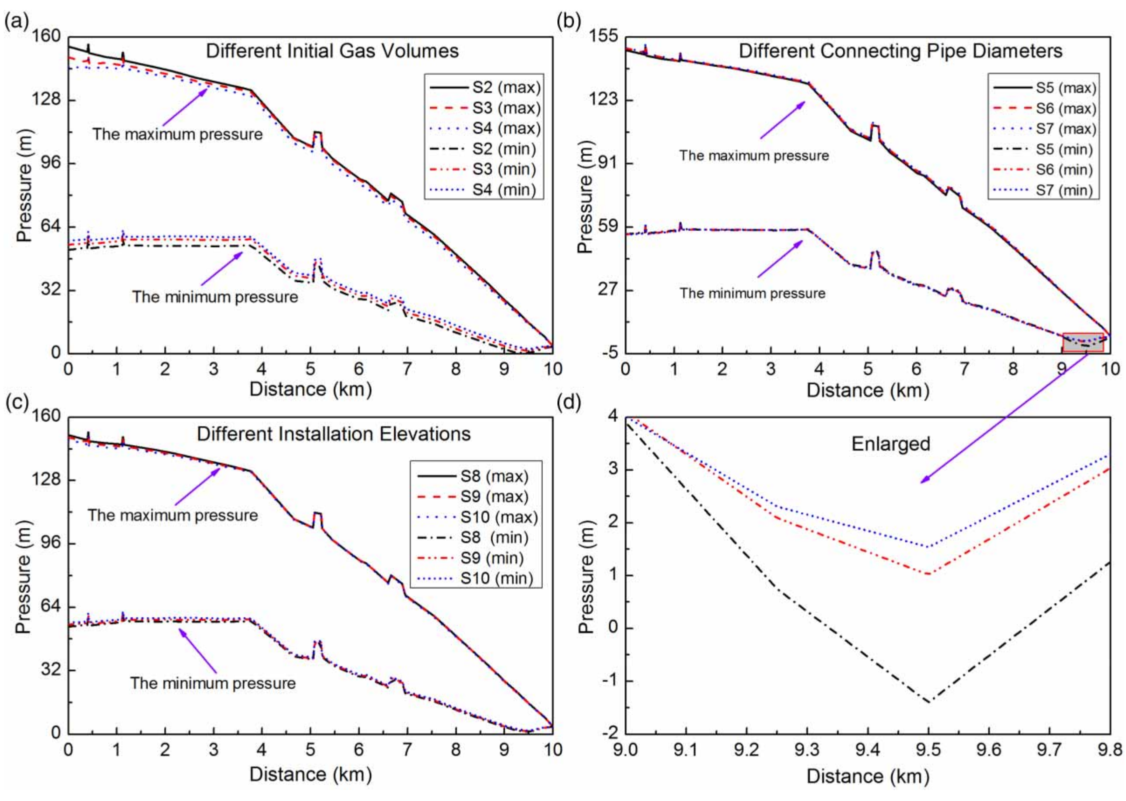

Figure 4 | Envelope curves of pressures along the pipeline for different spherical air vessels.

effect, at the expense of reducing the safety margin of the air vessel.

Figure 4(b) and 4(d) present the maximum and the minimum pressure along the pipeline as a function of both *d* and *distance*. In Figure 4(d), the maximum and the minimum pressures along the pipeline increased as the increase of the connecting pipe diameter. The calculations illustrate that increasing the connecting pipe diameter of the air vessel promotes negative water-hammer protection and inhibits positive water-hammer protection. The influence on the pipe pressure decreased with the increase of the connecting pipe diameter because the larger diameter of the connecting pipe is able to create smaller head losses during the outflow phase and thus reduce the negative pressure caused by the pump trip. Contrarily, the smaller diameter of the connecting pipe is able to produce larger head losses during the inflow phase and thus reduce the positive pressure caused by the water column coming back from the downstream. Hence, both the positive and the negative pressure standards of the pipeline should be considered when optimizing the connecting pipe diameter.

Figure 4(c) presents the maximum and the minimum pressures along the pipeline as functions of both *El* and *distance*. For a given parameter of the air vessel, the maximum pressure along the pipeline decreased from 152.30 m to 150.0 m and the minimum pressure increased from 1.25 m to 1.85 m when the installation elevation increased from 1,190.6 m to 1,196.6 m, as shown in Figure 4(c). The calculations imply that increasing the installation elevation of the air vessel has little effect on water-hammer protection. Therefore, for a given parameter of the air vessel, a suitable installation location can be selected according to the actual site layout.

CONCLUSION

A new spherical type of air vessel in a water supply system was proposed to protect from water-hammer waves. The protective effects of the cylindrical and spherical air vessels were studied and compared in different cases. A sensitivity analysis on the parameters of the spherical air vessel was performed. Based on the results, the main conclusions drawn were as follows.

The spherical air vessel performs better than the cylindrical air vessel in water-hammer protection. With the same protective effect on water hammer and safety margin, the spherical air vessel can effectively reduce the total volume and surface area compared with the cylindrical air vessel, thereby saving project investment as well as installation space. For a given volume of air vessel, using the spherical vessel, the gas initial volume in the vessel can be appropriately increased and a better protection effect can be obtained under the premise that the water in the vessel satisfies the requirement for water supply. Moreover, increasing the connecting pipe diameter of the air vessel is beneficial for negative water-hammer protection whereas it is detrimental for positive water-hammer protection. Finally, altering the installation elevation of the air vessel has little effect on water-hammer protection.

This study provides theoretical support for the application of the spherical air vessel in a long-distance water supply system. Further experiments on the protective effect of the spherical air vessel in a practical project are required in the future.

ACKNOWLEDGEMENT

This paper was supported by the National Natural Science Foundation of China (grant numbers 51879087 and 51709087) and the sponsorship of Jiangsu Overseas Visiting Scholar Program for University Prominent Youth & Middle-aged Teachers and Presidents.

REFERENCES

Bergant, A., Simpson, A. R. & Tijsseling, A. S. 2006 Water hammer with column separation: a historical review. *Journal of Fluids and Structures* **22** (2), 135–171.

Besharat, M., Viseu, M. T. & Ramos, H. M. 2017 Experimental study of air vessel behavior for energy storage or system protection in water hammer events. *Water* **9** (1), 63.

Chaudhry, M. H. 2014 *Applied Hydraulic Transients*. Springer, New York, USA.

Deng, A. L., Jiang, J., Lan, G., Fan, Z. & Liu, Z. 2015 Research on protective properties of air vessel for pump-stopping water hammer protection of long distance pipelines. *Engineering Journal of Wuhan University* **48** (3), 402–406 (in Chinese).

He, C., Zhang, J., Zheng, Y., Wang, Y. K. & He, D. Y. 2017 Protective properties of horizontal air vessel for water hammer. *Journal of Drainage and Irrigation Machinery Engineering* **35** (2), 138–143 (in Chinese).

Kim, S. G., Lee, K. B. & Kim, K. Y. 2014 Water hammer in the pump-rising pipeline system with an air chamber. *Journal of Hydrodynamics* **26** (6), 960–964.

Lee, T. S. 1998 A numerical method for the computation of the effects of an air vessel on the pressure surges in pumping systems with air entrainment. *International Journal for Numerical Methods in Fluids* **28** (4), 703–718.

Liang, X., Liu, M. Q., Zhang, J. G., Shen, Y. Z. & Lin, Q. 2005 Protection study on water hammer of pipelines by air vessel. *Drainage and Irrigation Machinery* **23** (6), 16–18 (in Chinese).

Miao, D., Zhang, J., Chen, S. & Li, D. Z. 2017 An approximate analytical method to size an air vessel in a water supply system. *Water Science and Technology: Water Supply* **17** (4), 1016–1021.

Perl, M. & Perry, J. 2010 The beneficial contribution of realistic autofrettage to the load-carrying capacity of thick-walled spherical pressure vessels. *Journal of Pressure Vessel Technology* **132** (1), 011204.

Stephenson, D. 2002 Simple guide for design of air vessels for water hammer protection of pumping lines. *Journal of Hydraulic Engineering* **128** (8), 792–797.

Sun, Q., Wu, Y. B., Xu, Y. & Jang, T. U. 2016 Optimal sizing of an air vessel in a long-distance water-supply pumping system using the SQP method. *Journal of Pipeline Systems Engineering and Practice* **7** (3), 05016001.

Wang, L., Wang, F. J., Zou, Z. C., Li, X. N. & Zhang, J. C. 2013 Effects of air vessel on water hammer in high-head pumping station. *IOP Conference Series: Materials Science and Engineering* **52**, 072010.

Wylie, E. B., Streeter, V. L. & Suo, L. S. 1993 *Fluid Transients in Systems*. Prentice-Hall, Inc., Englewood Cliffs, NJ, USA.

First received 4 November 2018; accepted in revised form 1 April 2019. Available online 17 April 2019